Biosensors and Bioelectronics 130 (2019) 382–388

Contents lists available at ScienceDirect

Biosensors and Bioelectronics

journal homepage: www.elsevier.com/locate/bios

Functional expression of olfactory receptors using cell-free expression system for biomimetic sensors towards odorant detection

Fangming Chen[a,1], Jian Wang[a,1], Liping Du[a], Xu Zhang[b], Fan Zhang[a], Wei Chen[a], Wen Cai[a], Chunsheng Wu[a,*], Ping Wang[c,*]

[a] Institute of Medical Engineering, Department of Biophysics, School of Basic Medical Sciences, Health Science Center, Xi'an Jiaotong University, Xi'an 710061, China
[b] Microbiology Institute of Shaanxi, Shaanxi Academy of Sciences, Xi'an 710043, China
[c] Biosensor National Special Laboratory, Key Laboratory for Biomedical Engineering of Ministry of Education, Department of Biomedical Engineering, Zhejiang University, Hangzhou 310027, China

ARTICLE INFO

Keywords:
Olfactory receptors
ODR-10
Biosensors
Cell-free expression systems
Electrochemical sensors

ABSTRACT

How to obtain sufficient functional olfactory receptors and coupled to transducers with high efficiency are crucial to biomimetic olfactory-based biosensors. In this study, a cell-free expression system was employed to prepare functional olfactory receptors that were utilized as sensitive elements for biomimetic olfactory receptor-based biosensors. A nematode olfactory receptor, ODR-10, was used as a model of olfactory receptors and expressed in *Escherichia coli (E. coli)* cell-free expression system. To improve the coupling efficiency and obtain the on-chip purification, a His_6-tag was expressed as a fusion to ODR-10, which makes the expressed ODR-10 capable of selectively binding to the sensor surface modified with anti-His_6-tag aptamers. Electrolyte-insulator-semiconductor (EIS) sensors were utilized as the transducer to measure the capacitance changes induced by the ODR-10 responding to its natural ligand, diacetyl. The results show that ODR-10 was successfully expressed using *E. coli* cell-free expression system and the expression could be promoted by adding 0.5% Brij58 as the detergent. Capacitance measurement results indicate that this olfactory receptor-based biosensor can detect diacetyl with high specificity and sensitivity. Concentration-dependent linear response to diacetyl ranging from 0.01 nM to 1 nM was obtained. The detection limit was as low as 0.01 nM. All the results demonstrated that the cell-free expression system provides a new approach for the preparation of functional olfactory receptors, which have great potential to be applied in biomimetic sensors towards chemical sensing.

1. Introduction

Olfaction is extremely important for the survival of the living such as feeding, mating, locating, avoiding natural enemies and identifying toxic substances (Buck and Axel, 1991; Gaillard et al., 2004). The biological olfactory system can detect a large number of different odors at the trace level benefited from the unique capability of olfactory receptors interacting with specific odorant molecules. Olfactory receptors are G-protein-coupled receptors (GPCRs) that can selectively bind to odorant molecules to activate intracellular signaling pathways and initiate a cascade of biochemical reactions, which can finally lead to the conversion of chemical signals of odorant molecules into electrical signals of olfactory sensory neurons (Dryer and Berghard, 1999; Lewcock and Reed, 2003; Reisert et al., 2005). As a result, olfactory receptors have been recognized as ideal candidates for the development of biomimetic olfactory-based biosensors for chemical sensing (Wu, 1999; Ko and Park, 2005; Sung et al., 2006; Kim et al., 2009; Yoon et al., 2009; Sankaran et al., 2011; Wu et al., 2012). Previous reports have demonstrated two main approaches for the preparation of functional olfactory receptors that are suitable to be used as sensitive elements in biosensors for odorant detection as summarized in a review (Du et al., 2013). One is to extract olfactory receptors from olfactory epithelium of living animals, which is an easy and convenient approach but suffered from the low abundance in the desire specific type of olfactory receptors and the consumption of a large number of living animals. The other one is to express specific olfactory receptors in a heterologous cell system, which can achieve desire functional olfactory receptors but suffered from the low expression efficiency due to the toxic effect of expressed olfactory receptors to the cell expression system. Therefore, it is highly desirable to explore new approaches for

* Corresponding authors.
E-mail addresses: wuchunsheng@xjtu.edu.cn (C. Wu), cnpwang@zju.edu.cn (P. Wang).
[1] These authors contributed equally.

https://doi.org/10.1016/j.bios.2018.09.032
Received 29 June 2018; Received in revised form 25 August 2018; Accepted 8 September 2018
Available online 10 September 2018
0956-5663/

the preparation of functional olfactory receptors in a more convenient and high-efficient manner.

Cell-free expression system provides an alternative approach for the preparation of functional olfactory receptors, which have great potential to overcome the limitations of current approaches mentioned above. Cell-free expression system uses exogenous mRNA or DNA as the template to synthesize target protein with the help of cell extract, energy mix and amino acid (Martemyanov et al., 2001; Kaiser et al., 2008; Wang et al., 2011). Cell-free expression system has attracted more and more attention due to their high efficiency in the expression of proteins that are difficult to express in heterologous cells, especially those of membrane proteins (Berrier et al., 2004; Kang et al., 2007; Gan et al., 2008). The decisive advantage of the cell-free expression system for the preparation of olfactory receptors is free of cell culture that avoids toxic cellular effects. In addition, cell-free expression system is easy to operate and regulate, which allows for the addition of detergent to improve the expression efficiency. Fusion expression of special labels is also feasible in the cell-free expression system, which facilitates the detection of production and purification of the expressed target receptor proteins. It is thus tempt to using cell-free expression system to prepare functional olfactory receptors for biomimetic sensors towards chemical sensing.

In this study, an *Escherichia coli (E. coli)* cell-free expression system was employed for the preparation of a nematode olfactory receptor, ODR-10 (Sengupta et al., 1996), which was used as a model of olfactory receptors and utilized as sensitive elements for biomimetic sensors towards chemical sensing. The optimal condition for ODR-10 expression was investigated and confirmed by western-blotting analysis. A His_6-tag was expressed as a fusion to ODR-10 to realize on-chip purification and immobilization of expressed olfactory receptors. To capture the expressed olfactory receptors onto the sensor surface, sensor surface was functionalized with anti-His_6-tag aptamers that can bind with proteins with His_6-tag. Electrolyte-insulator-semiconductor (EIS) sensors were used as transducers to measure the function of expressed olfactory receptors for the detection of specific odorant molecules via monitoring of the changes in sensor capacitance. The specificity and sensitivity of this biomimetic olfactory receptor-based biosensor for detecting odorant molecules were tested. It is worth to note that EIS sensors and olfactory receptors used in this study are only for demonstration of the technical feasibility of the new approach for the preparation of functional sensitive elements for chemical sensing.

2. Materials and methods

2.1. Construction of cell-free expression plasmids

Full-length cDNA of *odr-10* was amplified by PCR from *pBluescript SK⁻/odr-10* (provided by Professor Cornelia I. Bargmann at the Laboratory of Neural Circuits and Behavior, Howard Hughes Medical Institute, The Rockefeller University, NY, USA). The upstream and downstream primers are *5′- catgc catgg ctatg tcggg agaat tgtgg attac-3′* and *5′- cggga tcctt aatga tgatg atgat gatgc gtcgg aactt gagac aaatt g-3′* (Underline indicates *his_6-tag* sequence), respectively. PCR was performed in a 50 μL-reaction system using 2.5 U Pyrobest™ polymerase with 30 thermo cycles of 94 °C, denaturation for 30 s, 55 °C annealing for 1 min, and 72 °C extension for 1 min. The PCR product of *odr-10* full-length sequence was then subcloned into *pIVEX2.4c* digested with *BamH I* and *Nco I*. The *his_6-tag* sequence was inserted into the C-terminus of ODR-10. The sequence of cell-free expression plasmid *pIVEX2.4c/odr-10/his_6-tag* was confirmed by DNA sequencing. All the DNA sequences and enzymes were purchased from Takara (Japan).

2.2. Cell-free expression of ODR-10

An *Escherichia coli (E. coli)* cell-free expression system (RTP 100) purchased from Roche Molecular Biochemical (Switzerland) was utilized to express ODR-10. The constructed cell-free expression plasmid *pIVEX2.4c/odr-10/his_6-tag* was used as the template. 0.5 μg of *pIVEX2.4c/odr-10/his_6-tag* was introduced to a 50 μL cell-free expression system for the reaction at 30 °C for 4 h with a 400 rpm stirring speed. Brij58 was employed as the detergents to obtain soluble expression of ODR-10, which was introduced to the cell-free expression system at different concentrations to explore the optimal concentration for ODR-10 expression. To obtain the soluble fraction of expressed ODR-10, centrifugation was performed on the cell-free expression resulting solution at 10,000 × *g* for 10 min. The separated soluble fractions were used for further experiments. The western-blotting analysis was performed to test the soluble expression of ODR-10. The sample without plasmid addition (only H_2O) was loaded as the negative control. For the first, standard SDS-PAGE was carried out and the resulting gel was transferred to a PVDF membrane. After blocking, the membrane was blotted with mouse anti-his monoclonal antibody followed by HRP-conjugated goat anti-mouse IgG. The expression of ODR-10 was visualized using EZ-ECL Chemiluminescence Detection Kit for HRP. All the western-blotting related reagents were purchased from Beyotime (China).

2.3. Sensor preparation and functionalization

EIS sensors with a structure of Au/p-Si/SiO_2 were fabricated based on a p-type silicon wafer (< 100 >, 10–15 Ωcm) as schematically shown in Fig. 1. First, the silicon wafer was dry oxidized with a layer of SiO_2 with a thickness of 30 nm. Then, the rear side was etched with HF to remove SiO_2 and deposited with a layer of gold, which was used as an ohmic contact. Finally, the wafer was cut into pieces with sizes of 1 cm × 1 cm, which was then cleaned in an ultrasonic bath with acetone, isopropyl alcohol, ethanol, and deionized (DI) water before use.

Cell-free expressed ODR-10 was immobilized on the EIS sensor surface functionalized with 5′-end amino-modified anti-His_6-tag aptamer (5′-GCTAT GGGTG GTCTG GTTGG GATTG GCCCC GGGAG CTGGC-3′) that can specifically recognize and bind with His_6-tag. Aptamers were covalently immobilized on the sensor surface via silanization process with 3-aminopropyltriethoxysilane (APTES). Briefly, 0.1% (v/v) APTES in toluene was added to the cleaned sensor surface for 1 h incubation at room temperature (RT). After rinsed with toluene and ethanol three times, sensor surface was incubated with 2.5% glutaraldehyde for 12 h at RT. After rinsed with DI water and dried with a nitrogen stream, the sensor was incubated with the solution containing aptamers (10 μM aptamers, 0.1 M PBS, pH 8.5) for 12 h at RT. After washing, the sensor was treated with 1% bovine serum albumin (BSA)

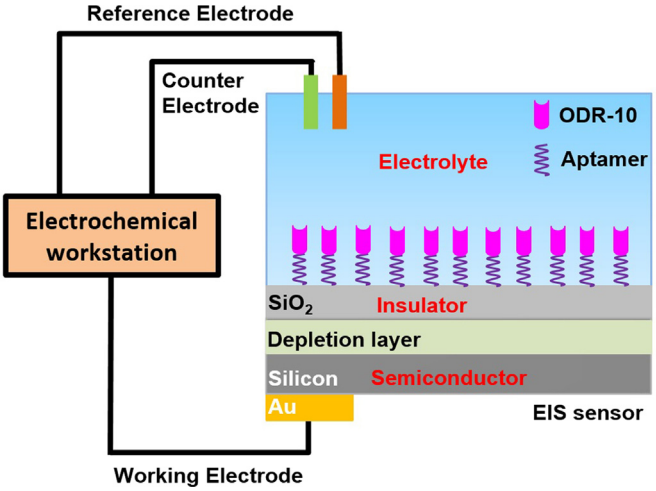

Fig. 1. Schematic diagram showing the structure of EIS sensor coupled with ODR-10 as an olfactory receptor-based biosensor.

solution for 30 min at RT to block unreacted aldehyde residues and other non-specific binding sites. Finally, the sensor was incubated with the cell-free expression resulting solution for 4 h at RT, which allows for the selective immobilization of the expressed ODR-10 fused with His_6-tag on the sensor surface. The EIS sensor functionalized with ODR-10 was stored at 4 °C for further experiments.

2.4. Electrochemical measurements

All the electrochemical measurements were carried out on an electrochemical workstation (Zennium, Zahner Elektrik, Germany) and used the Pt wire and Ag/AgCl (in saturated KCl) electrode as a counter electrode and a reference electrode, respectively (Fig. 1). For electrochemical measurements, the EIS sensor was fixed with a homemade measurement chamber and connected to the electrochemical workstation. Capacitance-voltage (*C-V*) and constant-capacitance (ConCap) measurements were employed to monitor the capacitance changes induced by surface modification steps for sensor preparation as well as interactions between ODR-10 and its ligands (Bronder et al., 2015). *C-V* measurements were performed by the application of a direct current (DC) gate voltage (− 0.5 V to + 1.5 V, steps of 100 mV) and a small superimposed alternative current (AC) voltage (20 mV, 60 Hz) to the EIS sensor via the reference electrode and the rear-side Au contact. ConCap measurements were carried out by varying the gate voltage using a feedback-control circuit to keep the capacitance constant at a certain working point, which is determined by the *C-V* curve (usually at 60% of maximum capacitance). ConCap measurement allows for the real-time dynamic monitoring of the sensor surface potential changes. All the measurements were performed in low-ionic strength measurement solution (5 mM PBS, pH 7.37) to reduce the influence of the charge-screening effect. All the measurements were performed at RT. The whole measurement chamber was shielded with a Faraday box to minimize the possible influence of ambient light and electromagnetic fields on the measurements.

3. Results and discussion

3.1. Cell-free expression of ODR-10

Olfactory receptors belong to the superfamily of GPCRs, which are membrane proteins containing 7 hydrophobic transmembrane domains (Sengupta et al., 1996). As a result, the expression of most membrane proteins in cell-free expression systems is insoluble and easy to precipitate due to their high hydrophobicity. In this study, a detergent, Brij58, was introduced to the cell-free expression system to increase the level of soluble and functional expression of the olfactory receptors. The underlying mechanism is due to the binding of detergent to the hydrophobic domain of the expressed integral olfactory receptors, which leads to the improvement in the soluble expression of olfactory receptors due to the reduction in their hydrophobicity (Berrier et al., 2004). However, too much detergent could result in the formation of large protein-detergent micelles and generate the expression inhibition effects. Therefore, in order to obtain the optimal concentration of Brij58 used for the expression of ODR-10 in *E. coli* cell-free expression system, different concentrations (0.25%, 0.5%, 1%, 1.5%, 2.0%, 2.5%) of Brij58 were investigated. The western-blotting results indicate that only a little amount of ODR-10 was soluble expressed when no detergent was added to the *E. coli* cell-free expression system as shown in the line 2 of western-blotting (Fig. 2). The addition of Brij58 in a certain range of concentrations (from 0.25% to 2%) can obviously improve the expression efficiency of ODR-10 as shown from line 3 to line 7 (Fig. 2). Among six different concentrations of Brij58, 0.5% Brij58 shows the highest improvement on the expression efficiency of ODR-10 as indicated by the white arrow in Fig. 2. However, the higher concentrations of Brij58 than 0.5% showed a downward trend in the improvement of ODR-10 expression efficiency. Therefore, 0.5% Brij58 was

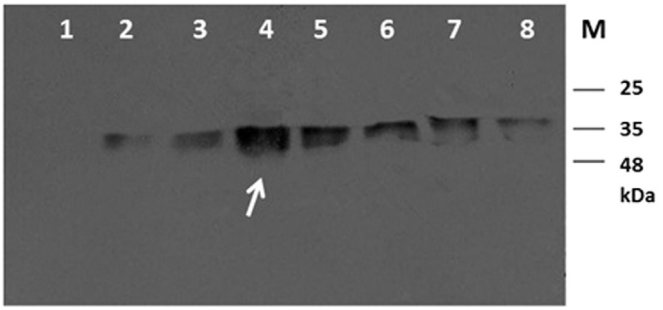

Fig. 2. The western-blotting result of the soluble expression of ODR-10 in *E. coli* cell-free expression system with different concentrations of Brij58. *lane 1*: negative control (only H_2O), *lane 2*: 0% Brij58, *lane 3*: 0.25% Brij58, *lane 4*: 0.5% Brij58, *lane 5*: 1.0% Brij58, *lane 6*: 1.5% Brij58, *lane 7*: 2.0% Brij58, *lane 8*: 2.5% Brij58, *M*: protein marker.

selected as the optimal detergent concentration for the expression of ODR-10 in *E. coli* cell-free expression system for further experiments. It is suggested that ODR-10 can be soluble expressed using *E. coli* cell-free expression system with proper detergent, which makes it suitable to be used as sensitive elements for biomimetic olfactory-based biosensors.

3.2. Selective immobilization of ODR-10 on the sensor surface

High-efficient coupling of olfactory receptors with transducers is of great importance to the performance of biomimetic olfactory-based biosensors. To improve the coupling efficiency of ODR-10 with EIS sensor, ODR-10 was fused with a His_6-tag, which makes it possible for ODR-10 to be selectively immobilized on the sensor surface modified with anti-His_6-tag aptamers. Therefore, other proteins without His_6-tag in the cell-free expression resulting solution can be easily removed from the sensor surface simply by washing. This allows for the on-chip purification of ODR-10, which could improve the coupling efficiency and consequently enhance the performances of the biomimetic olfactory-based biosensors. For this, surface silanization was carried out on EIS sensor surface using APTES, which is able to generate aldehyde group on the sensor surface. The aldehyde group can react with 5′-end amino-modified anti-His_6-tag aptamer, which allows for covalent immobilization of aptamers on the sensor surface. Water contact-angle measurements were employed to confirm the successful silanization of EIS sensor surface. DI water was utilized as the probe liquid to measure the contact angle before and after the surface silanization. As shown in Fig. 3, the measurement results show that the contact angle measured after silanization (Fig. 3b) is much higher than that of measured before silanization (Fig. 3a), which means that the sensor surface becomes more hydrophobic due to the formation of a self-assembled APTES layer (Wu et al., 2014). This suggests the success of the EIS sensor surface silanization. For the next, anti-His_6-tag aptamer was covalently immobilized on the EIS sensor surface, which was characterized by the fluorescent staining. As shown in Fig. 3c, FAM-labeled anti-His_6-tag aptamer was successfully immobilized on the EIS sensor surface with silanization. On the contrary, the EIS sensor surface without silanization shows no fluorescent signal, which indicates that no FAM-labeled aptamer was attached. These results demonstrate that the anti-His_6-tag aptamer was able to be covalently immobilized on the EIS sensor surface via silanization.

Atomic force microscopy (AFM) images were taken in tapping mode in the air with silicon cantilevers to characterize the attachment of ODR-10 onto the aptamer-modified EIS sensor surface. The images show that, compared with aptamer-modified EIS sensor surface (Fig. 4a), the surface after ODR-10 attachment (Fig. 4b) became rougher as indicated by the changes in root mean square (RMS), which increased from 0.645 nm to 1.807 nm. In addition, some small dots with diameters around tens of nanometers and height around 10 nm were

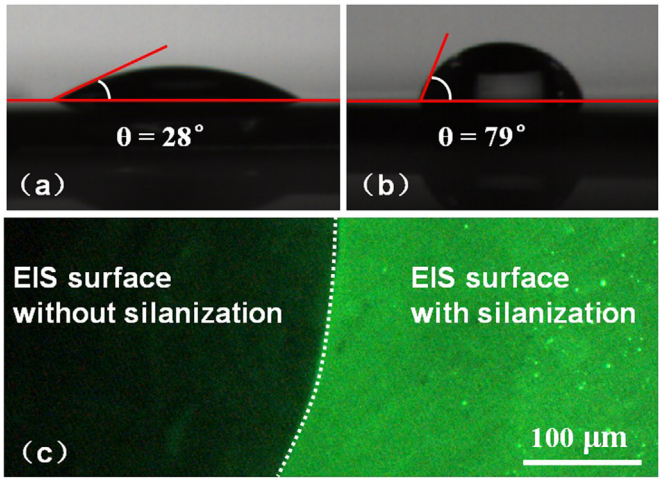

Fig. 3. Water contact-angle measured on an EIS sensor surface (a) before and (b) after silanization with APTES. (c) Fluorescence image taken from EIS sensor surface without and with silanization after exposing to FAM-labeled anti-His_6-tag aptamer. FAM: fluorescent dye carboxyfluorescein.

observed distributed almost evenly on the sensor surface, whose sizes were comparable to the sizes of olfactory receptor proteins. This is mainly due to the selective attachment of ODR-10 onto the aptamer-modified surface of EIS sensor since only cell-free expressed ODR-10 with His_6-tag can be captured by anti-His_6-tag aptamers and attached onto the sensor surface. These results indicate that ODR-10 were successfully coupled to the EIS sensor via the selective capture of anti-His_6-tag aptamers.

The attachment of ODR-10 onto the EIS sensor surface modified with anti-His_6-tag aptamers was further characterized by *C-V* and ConCap measurements, which are label-free capacitance-sensitive measurements sensitive to changes in sensor surface charges induced by the attachment of charged molecules (Bronder et al., 2015). Fig. 5 is an example of label-free electrostatic detection of anti-His_6-tag aptamer immobilization and ODR-10 attachment onto the EIS sensor surface using *C-V* and ConCap measurements. Fig. 5a shows the *C-V* curves recorded after silanization of EIS sensor surface, after anti-His_6-tag aptamer immobilization, and after ODR-10 attachment. It is indicated that the recorded *C-V* curves are typical high-frequency shapes, in which accumulation region, depletion region and inversion region can be obviously distinguished depending on the gate voltage applied to the EIS sensor. The shifts of *C-V* curves along the voltage axis can be observed in the depletion range after aptamer immobilization and ODR-10 attachment. It is indicated that an interfacial potential change was occurred due to the aptamer immobilization and ODR-10 attachment onto EIS sensor surface, which can thus lead to a modulation of the flatband voltage and changes in the capacitance of the EIS structure. In addition, the direction of the shifts is to the more negative gate voltage. This is in good agreement with the fact that aptamers and ODR-10 are negatively charged molecules, which will decrease the width of the depletion layer and increase the space-charge capacitance. Therefore, the *C-V* curve will shift to the more negative direction of gate voltages.

ConCap measurements were carried out to directly monitor and visualize the changes in the direction and the magnitude of potential shifts in a real-time manner. Fig. 5b is the dynamic ConCap measurement results obtained after silanization of bare EIS sensor surface, after anti-His_6-tag aptamer immobilization, and after ODR-10 attachment. The results show that a large potential shift around 153 mV to the more negative direction can be observed after incubation with solutions containing anti-His_6-tag aptamer. This potential change is mainly attributed to the immobilization of negatively charged aptamers on the EIS sensor surface. Similarly, ODR-10 attachment onto the EIS sensor surface lead to an additional potential shift around 43 mV to the more negative direction since ODR-10 is also negatively charged macromolecules. In general, as an average of measurement on 6 EIS sensors, the potential shifts induced by the aptamer immobilization and ODR-10 attachment on sensor surface were 151.3 ± 8.7 mV and 46.3 ± 5.8 mV, respectively. The potential shifts induced by the aptamer immobilization were much higher than that of caused by ODR-10 attachment. This could be explained by the assumption that (1) not all aptamers could capture ODR-10 due to the space-steric effect, (2) the charge density of ODR-10 is lower than that of aptamers, and (3) non-specific electrostatical adsorption of positively charged molecules or ions onto the EIS sensor surface, which could potentially result in the decrease of potential shift signals. All the results demonstrate that olfactory receptors were couple to the transducer with high efficiency. As summarized in Table S1, the time for olfactory receptor preparation using cell-free expression system is much less than that of using heterologous cell systems. On the other hand, the time for coupling of olfactory receptors with transducers is comparable to other olfactory receptor-based biosensors.

3.3. Detection of odorant molecules

To test the performance of this olfactory receptor-based biosensor for the detection of odorant molecules, different concentrations of diacetyl ranging from 0.01 nM to 100 nM were applied and the responses were monitored by *C-V* and ConCap measurements. Fig. 6a shows the zoomed *C-V* curves in depletion region recorded after exposure to different concentrations of diacetyl. It is indicated that the application of diacetyl leads to the shifts of *C-V* curves to the more positive direction of gate voltage. This is mainly attributed to the specific interactions between ODR-10 and diacetyl, which is the natural ligand of ODR-10. The specific interactions result in the conformation changes of ODR-10, which could lead to the redistribution of charges on the sensor surface and finally decrease the space-charge capacitance. As a result, the *C-V* curve will shift to the more positive direction of gate voltages. In addition, larger shifts in *C-V* curves were observed with the application of higher concentrations of diacetyl. Fig. 6b depicts the dynamic ConCap responses of this biosensor to different concentrations of diacetyl. It shows the higher concentrations of diacetyl induces a larger potential shift signals, which is in good agreement with the *C-V* measurement results. Fig. 7a is the statistical results of potential shifts of this olfactory receptor-based biosensor in response to diacetyl. The results show that a concentration-dependent linear response to diacetyl ranging from 0.01 nM to 1 nM was obtained. The detection limit of this olfactory receptor-based biosensor for the detection of diacetyl was as low as 0.01 nM, where a detectable potential shift signal of 12.6 mV has been registered.

The specificity of this olfactory receptor-based biosensor was tested by the application of different odorant molecules with similar chemical structures to diacetyl including butanone, 2, 3-pentanedione, and isopentyl acetate. EIS sensors with aptamer immobilization but without ODR-10 attachment were employed as the negative control. Fig. 7b is the potential shift responses of EIS sensors with and without ODR-10 attachment to different odorant molecules. When diacetyl was applied, the potential shifts of EIS sensors with ODR-10 attachment (16.5 ± 1.46 mV) are significantly higher than that of EIS sensors without ODR-10 attachment (3.1 ± 0.62 mV, $p = 5.81 \times 10^{-8}$, n = 6). The potential shifts of EIS sensors with ODR-10 attachment in response to diacetyl (16.5 ± 1.46 mV) is significantly higher than that of in response to 2, 3-Pentanedione (5.07 ± 0.88 mV, $p = 6.75 \times 10^{-6}$, n = 6). When other odorant molecules were applied, only very smaller potential shifts were observed no matter from the EIS sensors with or without ODR-10. The very smaller potential shifts observed are probably due to the non-specific adsorption of the odorant molecules attached onto the EIS sensor surface. These results suggest a good specificity of this olfactory receptor-based biosensor for the detection of diacetyl. Furthermore, this biosensor could be stored at 4 °C

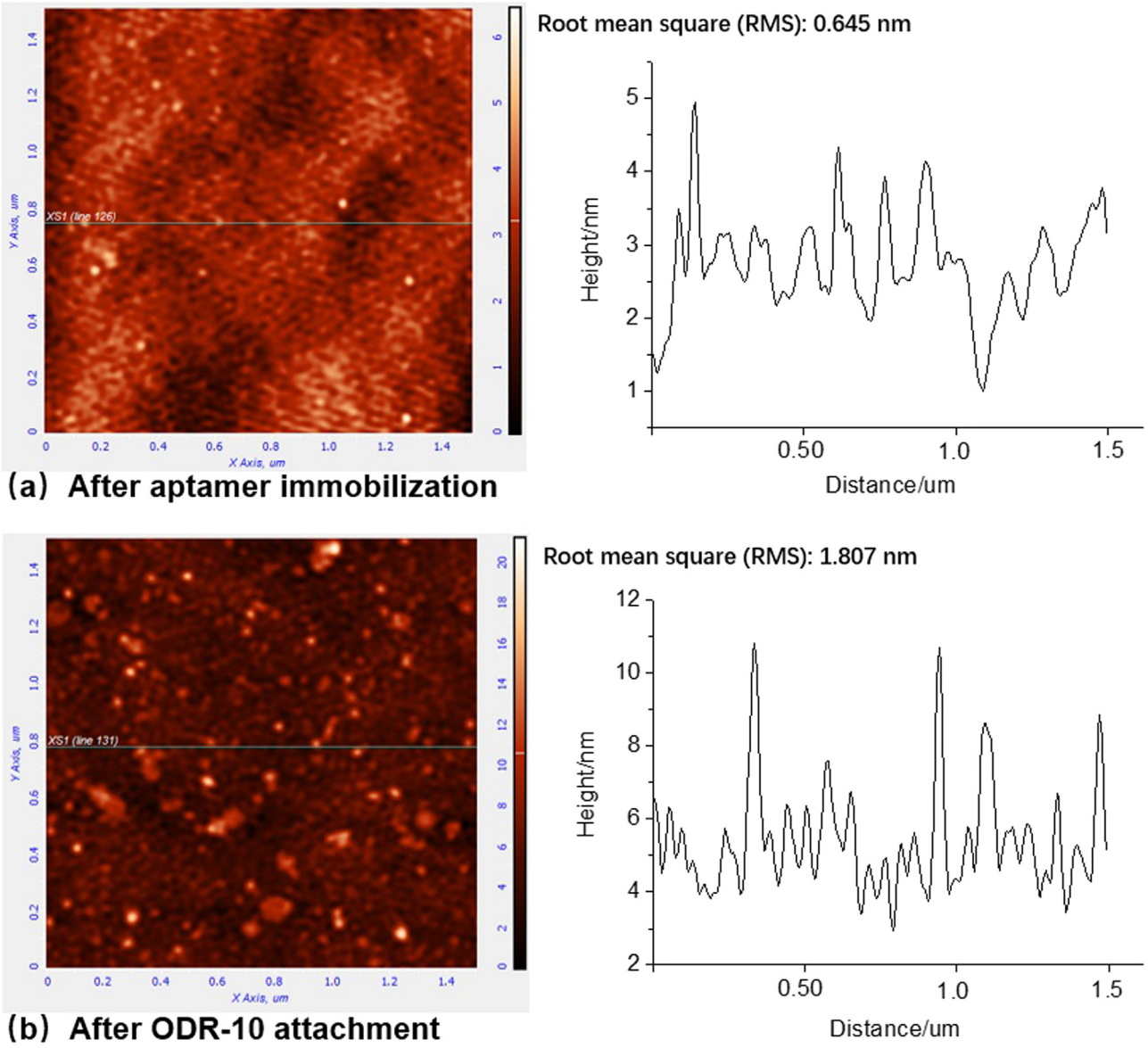

Fig. 4. AFM height images of (a) EIS sensor after immobilization of anti-His_6-tag aptamers and (b) after ODR-10 attachment onto the EIS sensor surface modified with anti-His_6-tag aptamers. Scan size is 1.5 μm × 1.5 μm.

in the dried chamber for 10 days without losing its response capability to diacetyl (data not shown), which demonstrated a good stability as an olfactory receptor-based biosensor.

4. Conclusions

In this work, the EIS sensor consisting of an Au/n-Si/SiO_2 structure functionalized with an olfactory receptor prepared by cell-free protein expression system has successfully been developed as an olfactory receptor-based biosensor and applied for the detection of specific odorant molecules. Cell-free protein expression systems provide a new approach for the preparation of functional olfactory receptors that are suitable to be utilized as sensitive elements for odorant detection. The cell-free expression system has shown decisive advantages such as free of cell culture, openness, and easy operation and regulation. *C-V* and ConCap measurements performed on EIS sensors can efficiently monitor the capacitance changes induced by the surface modification of charged molecules as well as the specific interactions between olfactory receptors and their ligands. This olfactory receptor-based biosensor shows linear concentration-dependent responses to specific odorant molecules ranging from 0.01–1 nM. The detection limit as low as 0.01 nM was obtained. Good specificity and stability of this olfactory receptor-based biosensor for odorant detection were also demonstrated. The obtained results also demonstrate the potential of the EIS sensor as promising transducer platform for developing molecular sensors towards label-free chemical sensing. Future work will be directed to develop multiple receptor-based biosensors to realize high-throughput detection of multiple odorant molecules.

Acknowledgments

This work was supported by the National Natural Science Foundation of China, China (Grant Nos. 31470956, 31661143030, 31700859, 31800827), the Doctoral Fund of Education Ministry of China, China (Grant Nos. 2016M602832, 2017M613146), and the Fundamental Research Funds for the Central Universities, China. The authors thank Prof. Bo Jiao's Research Group at Xi'an Jiaotong University, China for technical support.

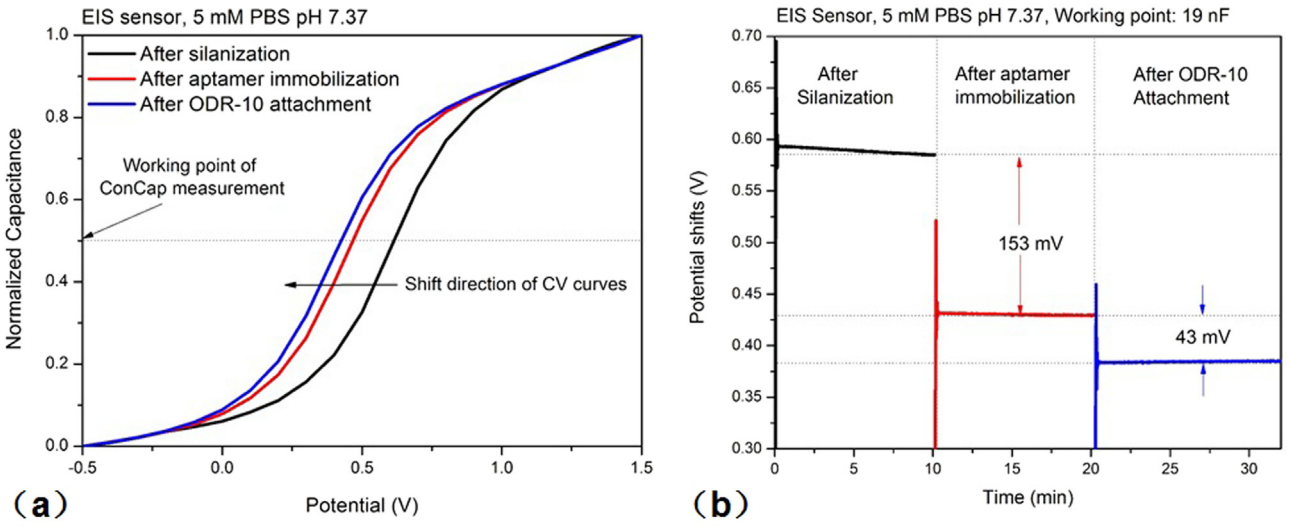

Fig. 5. Characterization of aptamer immobilization and ODR-10 attachment onto the EIS sensor surface using (a) shifts of *C-V* curves and (b) potential shifts of ConCap measurements. Working point of ConCap measurement was set to 19 nF.

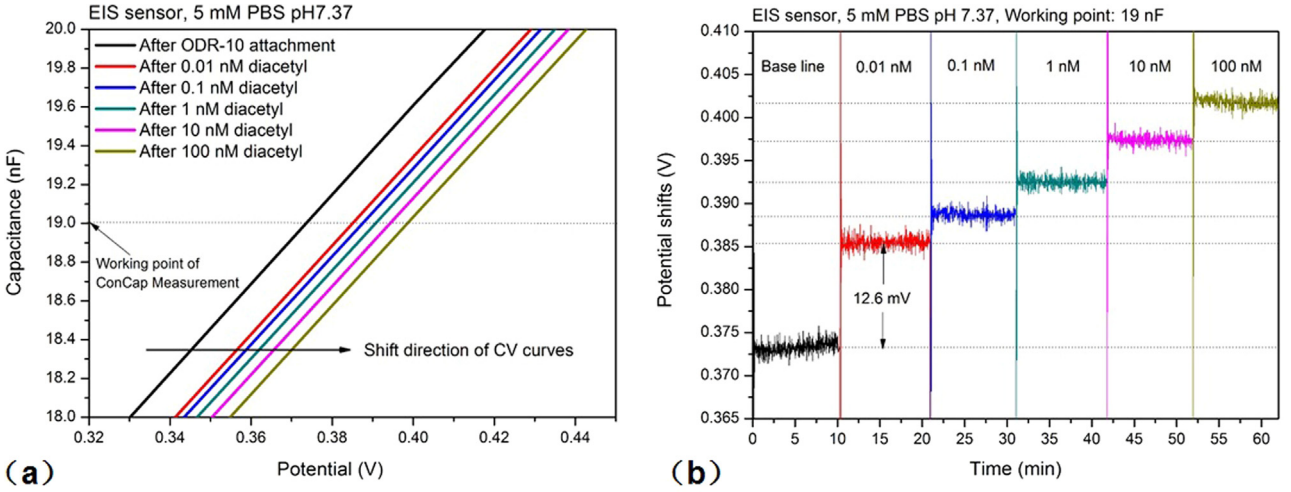

Fig. 6. Responses of the olfactory receptor-based biosensor to different concentrations of diacetyl ranging from 0.01 nM to 100 nM measured by (a) shifts of *C-V* curves and (b) potential shifts of ConCap measurements. Working point of ConCap measurement was set to 19 nF.

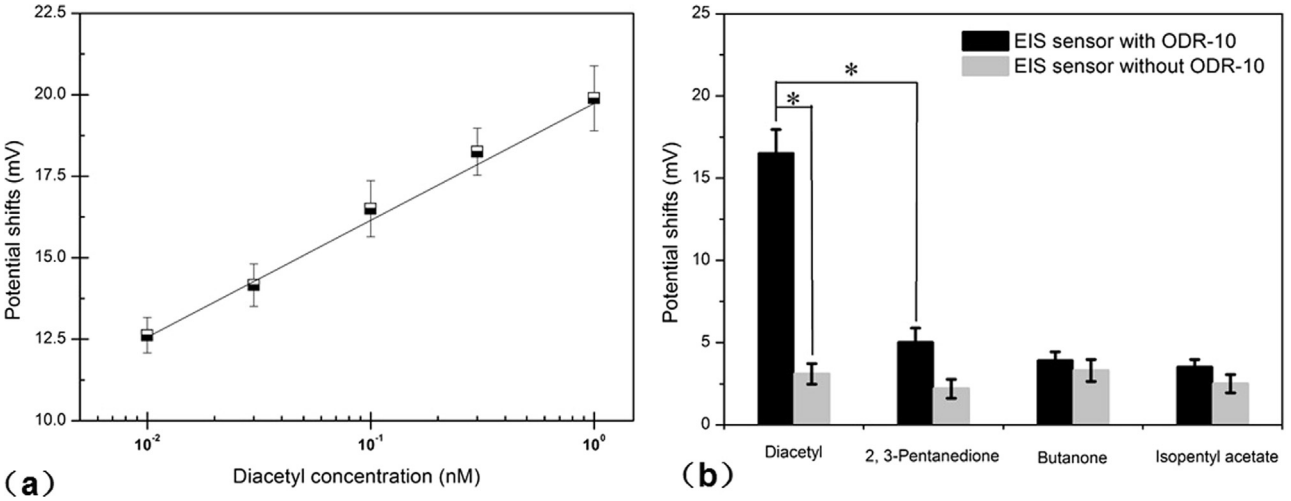

Fig. 7. (a) Statistical results of the olfactory receptor-based biosensor in response to serial concentrations of diacetyl (0.01 nM to 1 nM). The mean and stand error of the mean (SEM) of six experiments are shown ($N = 30$). (b) Statistical results of EIS sensors with and without ODR-10 attachment in response to different odorant molecules at the concentration of 0.1 nM. All data are represented by the mean ± SEM. $^{*}p < 0.01$, Student's *t*-test.

Appendix A. Supporting information

Supplementary data associated with this article can be found in the online version at doi:10.1016/j.bios.2018.09.032.

References

Berrier, C., Park, K.H., Abes, S., Bibonne, A., Betton, J.M., Ghazi, A., 2004. Biochemistry 43, 12585–12591.

Bronder, T., Poghossian, A., Scheja, S., Wu, C.S., Keusgen, M., Mewes, D., Schöning, M.J., 2015. ACS Appl. Mater. Interfaces 7, 20068–20075.

Buck, L., Axel, R., 1991. Cell 65, 175–187.

Dryer, L., Berghard, A., 1999. Trends Pharmacol. Sci. 20, 413–417.

Du, L.P., Wu, C.S., Liu, Q.J., Wang, P., 2013. Biosens. Bioelectron. 42, 570–580.

Gaillard, I., Rouquier, S., Giorgi, D., 2004. Cell. Mol. Life Sci. 61, 456–469.

Gan, R., Yamanaka, Y., Kojima, T., Nakano, H., 2008. Biotechnol. Prog. 24, 1107–1114.

Kaiser, L., Graveland-Bikker, J., Steuerwald, D., Vanberghem, M., Herlihy, K., Zhang, S., 2008. In: Proceedings of the National Academy of Sciences of the United States of America, vol. 105, pp. 15726–15731.

Kang, S.H., Jun, S.Y., Kim, D.M., 2007. Anal. Biochem. 360, 1–6.

Kim, T.H., Lee, S.H., Lee, J., Song, H.S., Oh, E.H., Park, T.H., 2009. Adv. Mater. 21, 91–94.

Ko, H.J., Park, T.H., 2005. Biosens. Bioelectron. 20, 1327–1332.

Lewcock, J.W., Reed, R.R., 2003. Science 302, 2078–2079.

Martemyanov, K.A., Shirokov, V.A., Kurnasov, O.V., Gudkov, A.T., Spirin, A.S., 2001. Protein Expr. Purif. 21, 456–461.

Reisert, J., Lai, J., Yau, K.W., Bradley, J., 2005. Neuron 45, 553–561.

Sankaran, S., Panigrahi, S., Mallik, S., 2011. Sens. Actuators B: Chem. 155, 8–18.

Sengupta, P., Chou, J.H., Bargmann, C.I., 1996. Cell 84, 899–909.

Sung, J.H., Ko, H.J., Park, T.H., 2006. Biosens. Bioelectron. 21, 1981–1986.

Wang, X.Q., Corina, K., Baaskec, P., Wienkend, C.J., Jerabek-Willemsend, M., 2011. Proc. Natl. Acad. Sci. USA 108, 9049–9054.

Wu, C.S., Bronder, T., Poghossian, A., Werner, C.F., Bäcker, M., Schöning, M.J., 2014. Phys. Status Solidi A 211, 1423–1428.

Wu, C.S., Du, L.P., Wang, D., Zhao, L.H., Wang, P., 2012. Biosens. Bioelectron. 31, 44–48.

Wu, T.Z., 1999. Biosens. Bioelectron. 14, 9–18.

Yoon, H., Lee, S.H., Kwon, O.S., Song, H.S., Oh, E.H., Park, T.H., Jang, J., 2009. Angew. Chem. Int. Ed. 48, 2755–2758.